Conformation and Phase Behaviour of Sodium Carboxymethyl cellulose in the Presence of Mono- and Di-Valent Salts

William N. Sharratt,[1] Róisín O'Connell,[1] Sarah E. Rogers,[2] Carlos G. Lopez,[3] and João T. Cabral[1]
[1)] *Department of Chemical Engineering, Imperial College London, London SW7 2AZ, UK*
[2)] *ISIS, Rutherford Appleton Laboratory, Harwell, Didcot, OX11 0QX, UK*
[3)] *Institute of Physical Chemistry, RWTH Aachen University, Landoltweg 2, 52056 Aachen, Germany*

We report a small angle neutron scattering (SANS) study of semi-dilute aqueous solutions of sodium carboxymethyl cellulose (NaCMC), in the presence of mono- (Na^+) and divalent salts (Mg^{2+}, Ca^{2+}, Zn^{2+}, Ba^{2+}). A degree of substitution of 1.3 is selected to ensure that, in salt-free solution, the polymer is molecularly dissolved with conformation well described by polyelectrolyte scaling theory in semi-dilute regime. We find that Na^+ and Mg^{2+} salt addition yield H-type phase behaviour, while Ca^{2+}, Zn^{2+}, and Ba^{2+} instead yield L-type behaviour, in decreasing order of the salt concentration associated with demixing. Charge screening by addition of Na^+ induces the progressive disappearance of the characteristic polyelectrolyte correlation peak and eventually yields scattering profiles with a q^{-1} dependence over nearly three decades in wavenumber q. By fitting a descriptive model to data with excess Na^+, we obtain a correlation length $\xi' = 1030 c_p^{-0.72}$ [Å] with polymer concentration c_p [g L^{-1}]. Addition of Mg^{2+}, which does not interact specifically with carboxylate groups, yields an analogous screening behaviour to that of Na^+, albeit at lower salt concentrations, in line with its higher ionic strength. At low salt concentration, addition of specifically interacting Ca^{2+}, Zn^{2+}, and Ba^{2+} yield a comparatively greater screening of the polyelectrolyte screening and, at concentrations above the phase boundary, results in excess scattering at low q, compatible with the formation of clusters of 10s nm in size. This behaviour is interpreted as due to the reduction in charge density along the chain, promoting association, clustering and eventual phase separation. Overall, drawing analogies with NaCMC at lower degree of substitution, where hydrophobic association takes place, our findings provide a framework to describe the solution conformation and phase behaviour of NaCMC in salt-free and salt solutions.

I. INTRODUCTION

Polyelectrolyte solutions, comprising charged polymer chains and oppositely charged counterions, are subject to long-ranged electrostatic repulsion which underpin their physical properties, such as solubility, viscoelasticity and phase stability. Polyelectrolytes in low ionic strength solution adopt highly extended conformations. They exhibit unique rheological behaviour and find use in a range of applications: from oil-recovery fluids to toothpastes and detergents.[1–4]

Electrostatic interactions in polyelectrolyte solutions underpin their phase behaviour and their conformation of chains in solution. Added low molecular weight salts reduce the interaction range through a reduction in the Debye-Hückel screening length (κ^{-1}), thereby imparting greater flexibility and a reduction in end-to-end distance of the chains, eventually becoming analogous to a neutral polymers. Mobile ions can impart more than simple charge screening: the size, valency, hydration and interaction type play an important in the phase behaviour and rheological properties of polyelectrolytes.[5] Particularly, multivalent ions can interact specifically with the polyelectrolyte and condense onto the backbone, reducing the charge density more effectively than monovalent ions. In their wide-ranging applications, polyelectrolytes may encounter a range of ions and understanding their phase behaviour and adopted conformation in the presence of such ions is crucial to further exploit these functional soft materials.[5–8]

In this study, we focus on carboxymethyl cellulose (CMC), generally used as a sodium salt (NaCMC), which is a semiflexible, weak, anionic polyelectrolyte, typically obtained by reacting cellulose with chloroacetic acid.[1,9–11] The number of carboxymethyl groups substituted at the hydroxyl position of the cellulose monomer (out of a maximum of 3) is known as the degree of substitution (D.S.), see Figure 1. We aim to establish the effect of added monovalent (Na^+) and divalent ions (Mg^{2+}, Ba^{2+}, Zn^{2+}, Ca^{2+}), on the phase behaviour and structure of NaCMC in semidilute solution (up to 35 g L^{-1}). We use turbidimetry to establish the phase boundaries before investigating the solution structure with Small Angle Neutron Scattering (SANS) in the single-phase and two-phase regions (turbid) regions of the polyelectrolyte-solution/added-salt phase diagrams. In doing so, we establish, for the first time, the conformation of semidilute NaCMC chains with added monovalent and divalent salts and discuss the origin of key features in their respective scattering patterns. We first begin with a discussion of the theory and current literature around scattering from polyelectrolyte solutions and polyelectrolyte phase

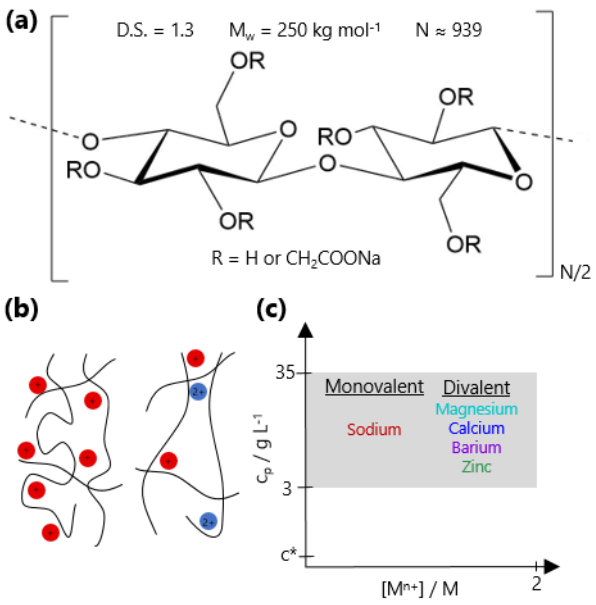

FIG. 1. (a) Chemical structure and characteristics of NaCMC used in this study. Two monomer units of NaCMC glycosidically linked. R = H corresponds to unsubstituted cellulose. The degree of substitution (D.S.) is the defined as the number R = CH_2COONa groups per monomer, out of a total of 3. The degree of polymerisation ($N \approx 939$) is determined from $M_w = 250$ kg mol^{-1} and $M_m \sim 266$ g mol^{-1}. (b) Schematic representation of hypotheses tested in this work; does additional monovalent salt increase chain flexibility in semidilute semiflexible polyelectrolyte solutions? Do multivalent ions create ion bridges which cause chain association? (c) Compositional envelope of semidilute NaCMC solutions with added salts, of varying types, investigated herein.

behaviour.

II. POLYELECTROLYTE SOLUTIONS: SCALING AND SCATTERING THEORY

A. Small Angle Neutron Scattering

The solvent subtracted, coherent, elastic scattering from a system containing polyelectrolyte, counterions and a single solvent can be written as follows:

$$I(q) = \rho[\bar{b}_m^2 S_{mm}(q) + 2\bar{b}_m\bar{b}_c S_{mc}(q) + \bar{b}_c^2 S_{cc}(q)] \quad (1)$$

$$I(q) \approx \rho\bar{b}_m^2 S_{mm}(q) \quad (2)$$

where $S_{ij}(q)$ is the spatial Fourier transform of density correlation function between scattering species i and j, often known as a partial structure factor. The corresponding contrast in scattering lengths are $\bar{b}_i$ and $\bar{b}_j$, respectively, and ρ is the number of monomers per unit volume. Here the scattering species, monomers (m) and counterions (c), have contrasts given by:

$$\bar{b}_i = b_i - b_s\frac{\bar{V}_i}{\bar{V}_s} \quad (3)$$

where b_i and b_s are scattering lengths of monomer/counterion and solvent, respectively, and $\bar{V}_i$ and $\bar{V}_s$ are the corresponding partial molar volumes. When dissolved in heavy water, the scattering length contrast arising from monovalent sodium counterions is ~ 6 % of polyelectrolyte contrast and therefore the dominant contribution to the total coherent scattering is the first term in Eq. 2.[12] We detail in SI Table II the partial molar volumes of species involved in this SANS study and corresponding scattering length contrast terms ($\bar{b}_i$) to further illustrate this point. Whilst the contrast between divalent ions and the solvent is larger than monovalent ions, at low added concentrations relative to the polymer the contribution to the overall scattering is again small. The monomer structure factor $S_{mm}(q)$ can be further decomposed into an intra- $S(q)$ and intermolecular $P(q)$ parts, often referred to as form and structure factors, and which account for the polyelectrolyte size and shape and interactions in solution, respectively:

$$S_{mm}(q) = S(q) + \rho P(q) \quad (4)$$

B. Polyelectrolyte Dimensions and Scaling Behaviour

In dilute solution, neutral polymer chains are isolated, unentangled and free from intermolecular inferences, and scattering can reconciled the single chain form factor. Upon increasing concentration the overlap concentration (c^*) is reached, where chains begin to interpenetrate and is given by: $c^* \simeq N/R^3 \sim N^{1-3\nu}$, where N is the degree of polymerisation and R is the polymer size in dilute solution. The chain dimensions vary as $R \propto N^\nu$, where ν is the solvent quality parameter. For $c > c^*$, the solution is termed semidilute and can be considered as a mesh of overlapping chains. The correlation length, the size of the mesh, is predicted to vary as:[13,14] $\xi(c) = R(c^*)\left(\frac{c}{c^*}\right)^{\nu/(3\nu-1)} \propto c^{-\nu/(3\nu-1)}$.

For polyelectrolyte chains, long-range Coulombic forces induce intermolecular correlations, even well below the overlap concentration ($c \ll c^*$). Scattering is almost always convoluted with a structure factor which is difficult to model analytically. Dobrynin's scaling model predicts that in dilute salt-free solution, chains are rod-like, corresponding to a solvent quality parameter of $\nu = 1$. Consequently, c^* is extremely small compared to neutral polymers[15] and we predominately observe polyelectrolyte solutions in the semidilute regime. Polyelectrolytes in salt-free solution display a correlation peak in their scattering profile at wavevector $q = q^*$, which is related to the correlation length by:

$$\xi \simeq 2\pi/q^* \quad (5)$$

In the semidilute regime, the correlation length is then expected to vary as $\xi \simeq (b/Bc)^{1/2}$, where b is the monomer length and B is a stretching parameter of order unity for semiflexible polyelectrolytes.[9]

C. Scattering Models

In excess salt, the reduction in the Debye-Hückel screening length (κ^{-1}) causes monomer charges to be screened and the chains are expect to behave like neutral polymers. Consequently the scattering profile of polyelectrolytes can be expected to follow an empirical correlation length model:[16]

$$I(q) \simeq \frac{I(0)}{1 + (q\xi)^{1/\nu}} \tag{6}$$

where $I(0)$ is the scattering intensity at $q = 0$. For neutral, flexible polymers in θ solvents, $\nu = 0.5$ and eq. 6 becomes the familar Lorentzian profile. For neutral polymers in good solvent ($\nu = 0.588 \simeq 0.6$), the scattering profile should remain unchanged for $q\xi < 1$, due to screening of excluded volume interactions at distances larger than ξ; for $q\xi > 1$, $1/\nu \simeq 5/3$ is expected, reflecting the expanded conformation in good solvent at distances smaller than ξ.

Horkay and co-workers have proposed an alternative descriptive expression to fit the scattering profile of semiflexible polyelectrolytes (biopolymers) in excess salt:

$$I(q) \simeq \frac{A}{q^m} + \frac{I_0}{[1 + (q\xi')^2]^{1/2}} P_{CS}(q) \tag{7}$$

where the first term describes the scattering of clusters and the second term for the polymer mesh, formed of rigid chains. $P_{CS}(q)$ accounts to the cross-sectional radius of the chains, and can be modeled by

$$P_{CS}(q) \simeq \left[2\frac{J_1(qR_c)}{qR_c}\right]^2 \tag{8}$$

where J_1 is a first order Bessel function of the first kind and R_c is the cross-sectional radius of the chain.

Where the structure factor is not prevalent in the scattering signal, typically in the high q region of the profile ($q \gtrsim 1/\xi$), the data can be fitted with:[9]

$$I(q)_{highq} \simeq \frac{I_0}{q} P_{CS}(q) \tag{9}$$

where $I_0 = \rho b_m^2 \pi / b'$, and b' is the effective monomer length ($b' = b/B$).

The small angle scattering from two phase systems may be interpreted through a version of the Debye-Bueche model and describes the spatial correlation between randomly distributed 2-phase systems.[17,18] The model takes the following form:

$$I(q) \simeq \frac{I_0}{[1 + (q\xi)^2]^2} \tag{10}$$

where $I_0 = 8\pi\phi(1-\phi)\Delta\rho^2\xi^3$ and ξ, $\Delta\rho^2$ and ϕ represent the correlation length and contrast between the two phases and the volume fraction of the 2-phase system. A linearised form of Eq. 10 takes the form:

$$\sqrt{\frac{1}{I(q)}} = \sqrt{\frac{1}{I_0}} + q^2\sqrt{\frac{\xi^2}{I_0}} \tag{11}$$

III. PREVIOUS WORK: POLYELECTROLYTE SOLUTIONS AND ADDED SALTS

A. Phase Behaviour

Phase diagrams for polyelectrolyte solutions in the presence of added salt are classified into two main categories;[19] H- and L-type. In H-type phase diagrams, phase separation occurs with large added salt concentrations ($\sim$ 1 M) and is associated with non-specifically interacting counterions, commonly monovalent ionic species such as sodium (Na^+). Phase separation for L-type behaviour occurs at much smaller concentrations of added salt ($\simeq$ mM).[20,21] L-phase diagrams exhibit further signatures and complexity: typically, the critical salt concentration required for phase separation is proportional to the polyelectrolyte concentration, reminiscent of mass action.[22–24]. Upon further reduction in polyelectrolyte concentration, the critical salt concentration can continue to decrease,[25–27] plateau,[28,29] or increase,[30–32] and is sensitive to the polyelectrolyte-salt mixture. While no systematic studies on the phase behaviour of carboxymethyl cellulose with divalent ions have been published, it is known that NaCMC displays L-type behaviour for most divalent cations except Mg^{2+}, which exhibits H-type phase behaviour, much like Na^+. Our interpretation of the literature leads to the hypothesis that H-type phase behaviour is driven by purely electrostatic screening and L-type phase behaviour arises from the entropically driven binding of specifically interacting counterions to the polyelectrolyte.[21,33] We therefore expect binding constants, or other thermodynamic binding data to predict the effect of different salts on polyelectrolyte solution phase behaviour. We find few studies have quantified the binding constant of divalent ions to carboxymethyl cellulose; Rinaudo *et al.* determined a degree of substitution dependent specific binding coefficient of Ca^{2+} over Na^+ on the order of 1×10^3,[34] Matsumoto *et al.* gave the ratio of divalent ions bound to CMC in the order $Mg^{2+} < Ba^{2+} \sim Ca^{2+}$,[35] and Haug *et al.* found $Mg^{2+} < Ca^{2+} < Ba^{2+} < Zn^{2+}$.[36] No clear correlations have been observed between phase behaviour of CMC and physical properties of the added divalent ions such as the atomic number or the Born radius.[5] Knowledge or expectation of the position of such phase boundaries, if present, do not, however, resolve the evolution of chain conformation as salts are added to the polyelectrolyte solution.

B. Conformation of Polyelectrolytes with Added Salts

Polyelectrolytes are known to be rigid on length scales smaller than their total persistence length (l_t), which is assumed to be comprised of an intrinsic ($l_{p,0}$) and electrostatic ((l_e) part. For cellulose and its derivatives $l_{p,0}$ can be large (34 - 206 Å)[37,38]. Several authors have developed models for so called worm-like chains, which are commonly used to fit light or neutron scattering data from polyelectrolytes.[39–41] Given the addition of a sufficient concentration of salt to screen the electrostatic contribution to the persistence length ($l_t = l_{p,0} + l_e$) the chains would be expected to behave as per a neutral semiflexible (or worm-like) chain. To the best of our knowledge, the few authors who have addressed semiflexible neutral polymers with scattering either remained in the dilute regime, and fitted with the Debye model or worm-like chain model,[42] or for semidilute solutions fitted an Orstein-Zernike expression.[43?]

The conformation of polyelectrolyte chains with added salt L-type mixtures has been addressed by a number of authors. Prabhu *et al.* investigated NaPSS-$BaCl_2$ mixtures by SANS; they showed that polyelectrolyte chains collapse as the phase boundary is approached but never reach the θ dimensions.[28,29] The correlation length diverges as the phase boundary is approached and the critical exponents were found to correspond to the 2D Ising universality class, suggesting high-salt polyelectrolyte solutions are similar to neutral polymer solutions. Hansch *et al.* investigated the conformation of single chains of NaPSS with Ba^{2+} and Al^{3+} counterions in the presence of monovalent by SAXS and SANS. They showed a decrease in the chain dimensions as the phase separation boundary was approached for both salt types but found compact domains only formed in the presence of Ba^{2+} and not Al^{3+}. Further SANS data by Dubois *et al.*[44] show that semidilute NaPSS in the presence of divalent and trivalent counterions can adopt a non-worm-like chain conformations, possibly due to local intra-chain electrostatic bridging, leading to an apparent chain 'thickening'.

Equation 6 has been used to accurately describe the small angle scattering signal of flexible polyelectrolyte NaPSS in excess monovalent,[45] or divalent salt solutions.[29] Dynamic light scattering (DLS) measurements of the hydrodynamic correlation length ξ_H of NaPSS in 0.01 M NaCl solution also shows $\xi_H \propto c_p^{-0.78\pm0.02}$.[46] The dependence of ξ_H on NaPSS concentration decreases as added NaCl concentration is increased to 0.1 M.[47] For semiflexible polyelectrolytes, Eq. 7 has been successfully used to describe the SANS profiles for a range of biopolymers in salt solutions.[48] They found the correlation length of semiflexible chondroitin sulfate and sodium hyaluronate in 0.1 M NaCl solution varies with polymer concentration as $\xi \propto c_p^{-0.65}$, in contrast to the expected scaling for polymers in good solvent $\xi \propto c_p^{-0.76}$ ($\nu = 0.588 \simeq 0.6$). For chondroitin sulfate, in the absence of salt $\xi_H \propto c^{-0.43}$ and in the presence of divalent salt $\xi_H \propto c_{CaCl_2}^{0.45\pm0.03}$.[49] The authors suggest that, in the absence of specific interactions, the ionic strength of added salt as a normalisation factor for the polyelectrolyte dependence of ξ_H. Geisser *et al.* used this relation that for semiflexible sodium hyaluronate in NaCl solution $\xi_H \propto (c/I)^{-0.75}$, where I is the ionic strength of the added salt, suggesting self-avoiding random walk statistics to describe the scaling of the concentration fluctuations in the system.[50,51]

IV. RESULTS & DISCUSSION

A. Phase Behaviour

H-type phase behaviour, where a high salt concentration ($\sim$ 1M) is required to induced phase separation and independently, is known for monovalent salt (Na^+) and divalent Mg^{2+} with NaCMC.[5] For other added divalent cations, we observe a complex dependence of the critical added divalent salt concentration, required to induce turbidity, on the polyelectrolyte concentration, as shown in Figure 2 (a). The dependence appears similar irrespective of salt type (for Ca^{2+}, Ba^{2+}, Zn^{2+}). At low NaCMC concentrations, the salt concentration required to induce phase separation ($c_{s,0}$) is independent of NaCMC concentration and is specific to each salt. Upon increasing NaCMC concentration, past a critical value ($c_p{}^*$), the critical salt concentration becomes linearly dependent on NaCMC concentration with a dependence denoted by c_s/c_p. The values of $c_{s,0}$, $c_p{}^*$ and c_s/c_p are given in Table I. As visible in Figure 2, Ca^{2+} has the highest $c_{s,0}$, followed by Zn^{2+} and then Ba^{2+}. A similar ordering can be seen with $c_p{}^*$ and c_s/c_p. The crossover concentration, $c_p{}^*$, always appears at a concentration of $c_p \geq c_{s,0}$.

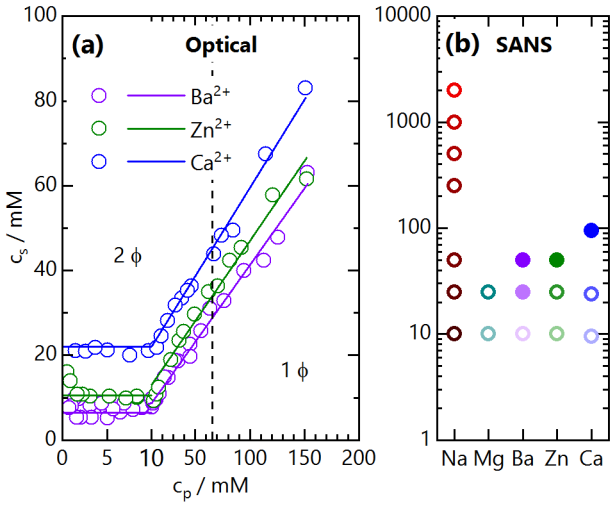

FIG. 2. (a) Phase separation boundary, determined optically, of salt-free NaCMC solutions upon addition of divalent salt. The data are plotted as molar concentrations of added salt (c_s) against molar concentration of monomer units c_p. Lines are linear fits to the data for which the salt concentration required to induce precipitation is independent of c_p for $c_p \lesssim 10$ mM and proportional to c_p for $c_p \gtrsim 10$ mM. The horizontal axis contains a break at 10 mM and a change in scale. (b) Compositions probed with SANS at constant $c_p = 17.1$ g L^{-1} $\approx$ 64 mM and with various added salt types and concentration. Added salt concentration is indicated on a log scale and 2 phase samples are indicated by filled symbols.

The mixed L-type phase behaviour observed with NaCMC and added Ca^{2+}, Zn^{2+}, Ba^{2+} cannot be reconciled solely with electrostatic contributions from the divalent ions to the ionic strength of solution. We interpret the relative positions of the phase boundaries and parameters in Table I as indications of the relative binding strengths of each divalent ion to NaCMC. Whilst Na^+ and Mg^{2+} exhibit H-type phase behaviour and are the most weakly binding divalent studied here, the ordering of other ions does not directly correlation with literature values of the binding of divalent ions to NaCMC as we deem Ba^{2+} the most strongly binding ion (by the lowest observed phase boundary).[35,36] Our results follow the trend identified by Schweins *et al.* who for sodium poly(acrylate) (NaPA) in the presence of alkaline earth cations.[26] For NaPA with a fixed concentration of inert NaCl, they find L-type phase behaviour upon addition of divalent ions (Ca^{2+}, Sr^{2+}, Ba^{2+}). The slopes and intercept of their phase boundary decrease as the periodic table is descending in the group II alkaline earth metals. Numerous authors have suggested precipitation occurs when a certain fraction of divalent ions are bound to the polyelectrolyte,[23,52] reducing the charge density, promoting aggregation and eventual precipitation. From our measurements, we expect that Ba^{2+} binds the most strongly to NaCMC. We attempted to model our phase behaviour using an approach from Axelos *et al.*, in terms of the critical fraction of bound ions and ion binding constants, illustrated in SI Figure 12. The model reproduces some of the features of the phase boundaries but yields values for the free parameters which are inconsistent with our observed order of phase boundaries with salt type. Knowledge of the phase boundaries with added divalent salts is then used to determine the compositions to be investigated with SANS and are illustrated in Figure 2 (b).

Cation	$c_{s,0}$ / mM	$c_p{}^*$ / mM	c_s/c_p
Ca^{2+}	21.5 $\pm$ 0.5	15 $\pm$ 2	0.416 $\pm$ 0.010
Zn^{2+}	10.5 $\pm$ 0.5	12 $\pm$ 2	0.377 $\pm$ 0.016
Ba^{2+}	6.5 $\pm$ 1.5	7 $\pm$ 3	0.362 $\pm$ 0.007

TABLE I. Phase diagram parameters for NaCMC in the presence of various cations. $[M^{2+}]_0$ is the salt concentration at which precipitation occurs at low polymer concentrations, $c_p{}^*$ is the polymer concentration at which an inflection point is observed in the Figure 2 and c_s/c_p is the slope of the phase diagram in the high polymer concentration region.

B. Small Angle Neutron Scattering

1. Salt-Free Solutions

We first illustrate the small-angle scattering from NaCMC solutions in the absence of added salt, as shown in Figure 3. Both SANS (a) and SAXS (b) demonstrate the expected scattering from a salt-free polyelectrolyte solution, characteristic by a broad polyelectrolyte peak. Mean-field approaches are known to not hold given the strong-electrostatic coupling.[53] SAXS measurements extend the range of concentrations, previously studied by

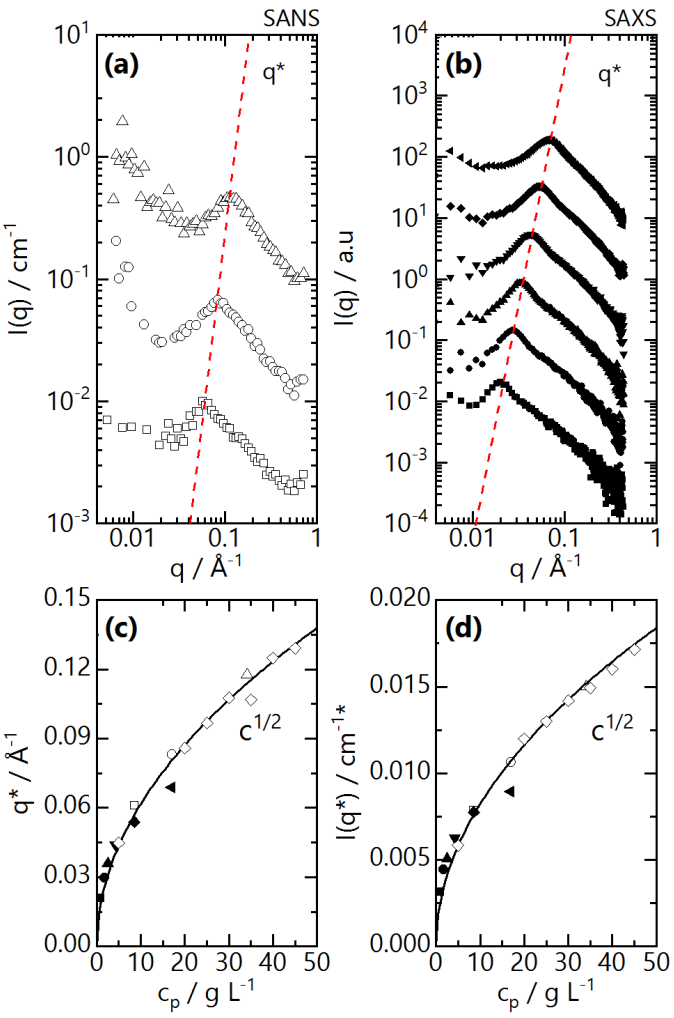

FIG. 3. Small angle scattering for NaCMC in salt-free solution. Background subtracted scattering intensity as a function of q for SANS (a) and SAXS (b) experiments. NaCMC concentrations: (a) 8.5 (□), 17.1 (○), 34.2 (△) g L^{-1} and (b) 0.85 (■), 1.7 (●), 2.6 (▲), 4.3 (▼), 8.5 (♦) 17.1 (◄) g L^{-1}. Data in (a) and (b) are offset 5X relative to the lowest concentration in each case. (c) Peak position (q^*) and (d) scattering intensity ($I(q^*)$) as a function of polymer concentration. SAXS values for $I(q^*)$ are shifted by an arbitrary constant to match SANS values. Lines are the square-root concentration dependence predicted by scaling theory. In (c) and (d), open diamonds are data taken from Ref. [9] for NaCMC with D.S. = 1.2 and M_w = 250 kg mol^{-1}.

Lopez *et al.*[9] with SANS, to 0.85 g L^{-1} $\simeq$ 3 mM NaCMC. We observe clustering leading to an upturn in the low q region ($q < 0.01$ Å^{-1}) and a correlation peak q^*, with intensity $I(q^*)$ and a q^{-1} dependence for $q > 1.5q^*$. q^* and $I(q^*)$ increase with increasing concentration, as shown in Figure 3 (c) and (d), respectively. From SANS we recover $I(q^*) = (2.81 \times 10^{-3} \pm 0.14 \times 10^{-3})c^{-0.47\pm0.02}$ cm^{-1} and $q^* = (0.0216 \pm 0.001)c^{-0.48\pm0.02}$Å^{-1} which, through Eq. 5, yields $\xi = (283\pm18)c^{-0.47\pm0.02}$Å (with c in g L^{-1}). Dobrynin's scaling theory predicts $\xi = (B/bc)^{1/2}$,[54] where b= 5.15Å for a cellulose monomer, and from our extracted correlation length dependence yields stretching parameter $B = 1.12 \pm 0.07$, which is entirely consistent with rod-like, rigid chains for q > $1/\xi$, and with previously established stretching parameters for NaCMC with D.S. in the range $0.7 \lesssim$ D.S.$\lesssim 1.2$.[9,55] From SAXS we recover a slightly weaker dependence of q^*, $I(q^*)$ and ξ on c. $q^* = (0.0232 \pm 6 \times 10^{-4})c^{-0.41\pm0.03}$Å^{-1} yielding $\xi = (270 \pm 8)c^{-0.42\pm0.03}$Åand $B = 0.85 \pm 0.03$, and $I(q^*) = (0.0231\pm7\times10^{-4})c^{-0.38\pm0.03}$ cm^{-1}. Fits of Equation 9 to data in Figure 3 (a) and (b) resolve the chain radius which we establish as $R_{c,SANS} = 3.8 \pm 0.6$ and $R_{c,SAXS} = 4.9 \pm 0.8$ Å across the concentration range here, which agrees well with a previous study.[9] The larger SAXS chain cross-section corresponds to the contrast arising from the diffuse sodium counterion cloud and $\simeq 1$ Åradius of the sodium ion. Overall, our measurements of salt-free NaCMC by SAXS and SANS are consistent with previous reports on salt-free NaCMC,[9] and other salt-free semidilute polyelectrolyte solutions.[56–58]

2. Monovalent Salt

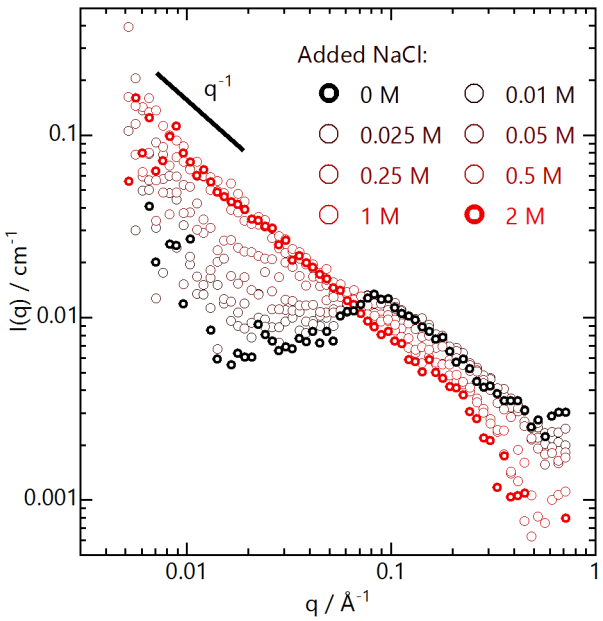

FIG. 4. Coherent SANS profiles for 17.1 g L^{-1} ($\sim$ 64 mM) NaCMC with 0-2 M added NaCl. The correlation peak disappears between 0.05-0.25 M and a q^{-1} dependence appears at $q < 0.1$ Å^{-1}.

Upon addition of monovalent salt, the Debye screening length decreases as $\kappa^{-1} \propto c_s^{-0.5}$. The effect of screening the long-range inter-chain correlations on the SANS profiles for 17.1 g L^{-1} ($\sim$ 64 mM) NaCMC with 0 - 2 M added NaCl is shown in Figure 4. Upon addition of small amounts of NaCl ($c_s < c_p \simeq$ 64 mM), the correlation peak is still apparent and with a position q^* which ap-

pears invariant to c_s. Whilst some authors have observed q^* shift to lower q values upon presence of monovalent salt,[59–63] several authors have observed the same invariance with addition of NaCl to salt-free polyelectrolyte solutions.[58,64,65] The scattering intensity around $q \leq 0.01$ Å^{-1} increases with added salt and causes disappearance of the correlation peak between $c_s = 0.05-0.25$M ($\approx c_p$). The change in added salt corresponds to a decrease in the Debye-Hückel screening length (κ^{-1}) from $\simeq 14$ Åto $\simeq 6$ Å, which becomes commensurate with the distances between charges on adjacent monomer units.[66] Our results cannot conclude whether the c_s at which correlation peak is screened corresponds to the plateau in effect of c_s has on the solution viscosity,[15,67] which is expected at ≈ 0.1 M for NaCl.

On further salt addition (0.5, 1 and 2 M), a q^{-1} dependence is recovered across almost 3 decades of wavevector q. In 2 M excess salt, we do not recover a profile resembling a semiflexible neutral polymer which can be fitted an Ornstein-Zernike type expression.[42,68] We observe a reduction in scattering intensity at high q (≥ 0.1 Å^{-1}) by $\approx 1/3$ once more than 1 M NaCl is added. As the absolute intensities are near the typical resolution ($\simeq 10^{-3}$ cm^{-1}) of SANS instruments, we cannot reconcile the differences with changes in the partial molar volume of the polyelectrolyte and resulting contrast factor despite expectations that as electrostatic interactions are screened, chain dimensions should shrink. Our density measurements, shown in SI Figure 13, actually reveal an increase in the apparent molar volumes of NaCMC with increasing NaCl concentration. The solutions appear homogeneous and the decrease in high-q scattering intensity cannot be reconciled with a loss in concentration of chains from solution. We also find an isoscattering point, where scattering intensity remains constant as salt concentration is increased, at $q = 0.071$ Å^{-1} which corresponds to a real space distance $\simeq 89$ Å. The origin of isoscattering points in non-dilute, polydisperse systems is unclear.[69] The number of isoscattering points appearing with the small angle q-range ($10^{-3} - 0.6$Å) is indicative of the shape of scattering 'particle', typically for micelles, and speculatively in this instance could be indicative of the electrostatic blob size.

Figure 5 (a) shows offset coherent SANS profiles for 0.25 - 2 M NaCl with fits to Equation 7. We chose to fit the lowest possible correlation length in the model as profiles exhibiting a q^{-1} dependence could be fitted with a large range of unphysical values of correlation length (ξ') and prefactor (I$_0$). We defined here the correlation length ξ', as the physical origin is expected to differ from the mesh size established for salt-free polyelectrolyte solutions (in Equation 5). We ignore the effect of any clustering which is clearly observed for $c_s \leq 0.25$ M, which can again result in unphysical ξ' and I$_0$ values. We observe that the model from Horkay *et al.* provided good fits to the data over the full q range at higher added salt concentrations, despite not seeing a plateau at low q, and owing to the presence of the correlation peak at lower salt concentrations. Both the prefactor and correlation length extracted from the model, shown in Figure 5 (b) respectively, increase with added monovalent salt. Solid and dashed lines indicate a power law dependence of both variables on the added salt concentration. $\xi' = (75 \pm 6)c_s^{0.75\pm0.12}$ Å and $I_0 = (0.068 \pm 0.005)c_s^{-0.63\pm0.12}$ cm^{-1}.

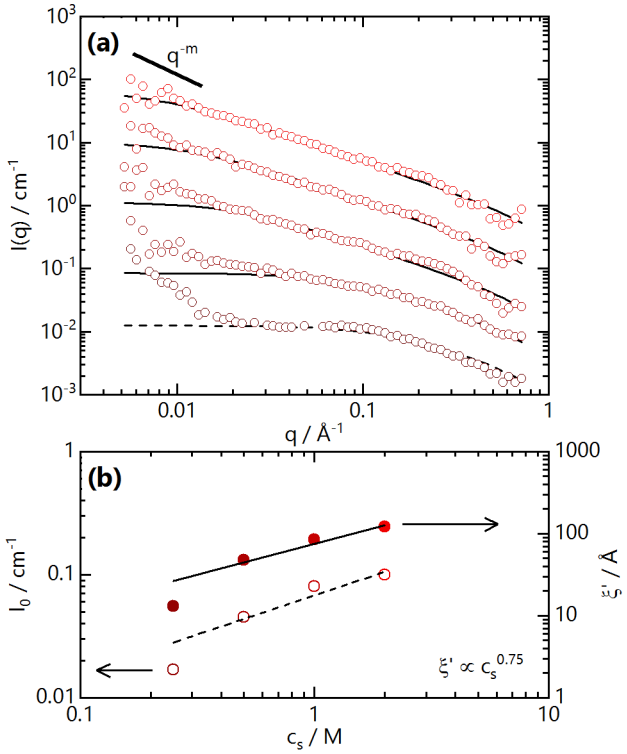

FIG. 5. (a) Offset (5X) coherent SANS profiles for 0.05 - 2 M added NaCl. Lines are fits to Equation 7 (b) Log-log plot of I_0 (left axis) and ξ' (right),extracted from fits in (a), as a function of added salt concentration (c_s).

Given the q^{-1} dependence, which emerged with increasing added monovalent salt, we investigated whether this behaviour was consistent over a concentration range of NaCMC in excess salt. In 2 M NaCl we probed an accessible c_p/c_s range $\simeq 0.01 - 0.06$ by varying c_p from $\simeq 5.1-34.2$ g L^{-1} ($\sim$ 19.3 - 129 mM). Figure 6 (a) shows offset SANS profiles for NaCMC in 2 M NaCl with fits to Eq. 7. All profiles exhibit a $I \sim q^{-1}$ dependence over the majority of the the q range measured. We observe, at high q (~ 0.6 Å^{-1}), deviation from q^{-1}, owing to the sensitivity of the scattering intensity to the background subtraction and the scattering contribution of chain cross section, which is still weak for our highest concentrations. The data collapse when scaled by their respective concentrations, as shown in Figure 6 (b), highlighting a concentration invariant q^{-1} dependence. The prefactor and correlation length extracted from the fits to Equation 7 are shown in Figure 6 (c) and (d), respectively. Both follow power law dependence on c_p: $I_0 = 0.051\pm0.008$ c$_p^{0.30\pm0.05}$ cm^{-1} and ξ'$= 1030 \pm 190$c$_p^{-0.72\pm0.08}$ Å. The concentra-

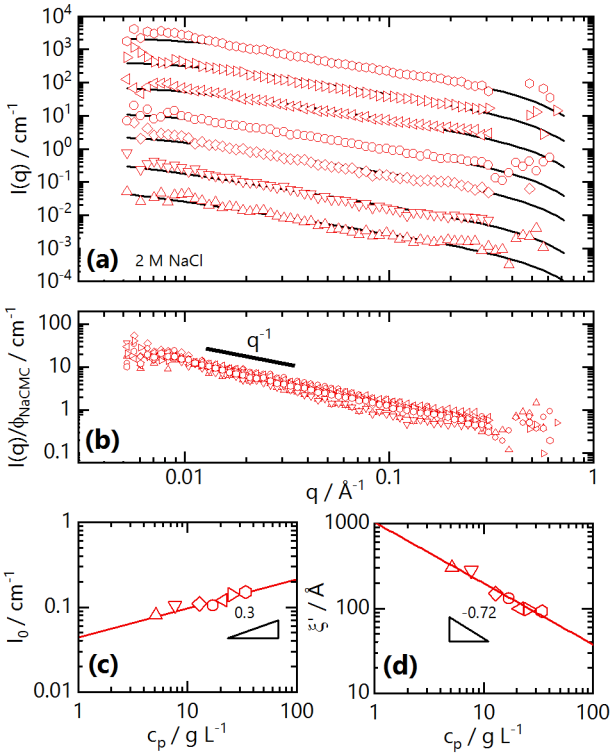

FIG. 6. (a) Coherent SANS profiles from 5.1 (△), 7.7 (▽), 12.8 (◇), 17.1 (○) 21.4 (◁) 25.6 (▷) and 34.2 (⬡) g L^{-1} NaCMC in 2 M NaCl solution. Profiles are offset by 5x with increasing concentration and are referenced to 3.4 g L^{-1}. (b) Coherent SANS profiles from (a) scaled by volume fraction of NaCMC. Log-log plots of Eq. 7 prefactor I$_0$ (c) and correlation length ξ (d) as a function of NaCMC concentration.

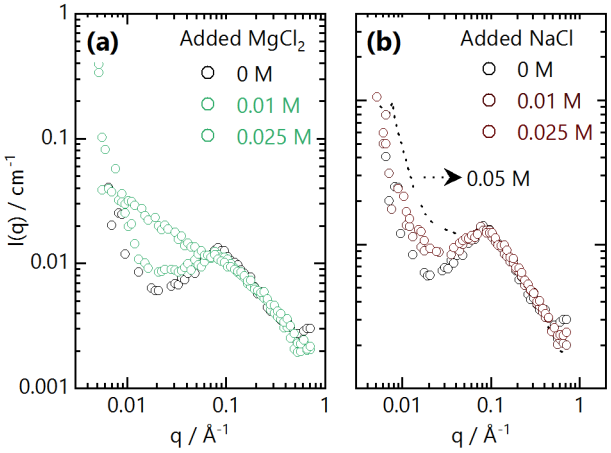

FIG. 7. Direct comparison of the SANS profiles from 17.1 g L^{-1} (∼ 64 mM) NaCMC with added Mg^{2+} (a) and Na^{+} (b) salts. All compositions lie within the homogeneous region of their H-type phase diagram.

tion dependencies of both I_0 and ξ' are consistent with the asymptotic form of Equation 7 which should yield $I_0/\xi' \propto c^1$. The fitted I_0 values are also consistent with those fitted for constant c_p and varying c_s. The fitted correlation lengths in excess salt are $\sim 1.5 - 2.5$ times the correlation length in salt-free solution, reflecting the screened electrostatics and greater spatial extent of concentration fluctuations.

The calculated dependence of ξ' on c_p in excess salt (2 M) does not agree with the expectation for rod-like polymers.[70] Instead of $\xi' \propto c^{-1/2}$, we recover the expected scaling for semidilute neutral flexible polymers in good solvent ($\propto c_p^{-0.75}$). A previous study on a number of semiflexible polyelectrolytes in semidilute solution with added NaCl (0.1 M) found the exponent to be instead $c_p^{-0.65\pm0.05}$, which, despite the salt concentration not being in vast excess, roughly agrees with our results.[48] Both results are entirely consistent with Odijk's scaling theory,[71] and suggests that NaCMC (and semiflexible polyelectrolytes) in excess salt adopt a solution structure where chains are rigid for $q > 1/\xi$' whilst adopting a self-avoiding random walk of electrostatic blobs for $q < 1/\xi$'.[72] The fitted prefactor, which is indicative of the osmotic compressibility of the solutions, would be expected for neutral polymers in good solvent to yield $I_0 \propto c^{-1/4}$, whereas we find an exponent of roughly the same magnitude but opposite sign. This could be a feature of added polyelectrolytes within the semidilute regime contributing to the ionic strength and effectively screening the bare charges, leading to a recovery in osmotic compressibility.

The recovered scaling for NaCMC at fixed c_p and varying c_s, however, disagrees with Odijk scaling approach, which predicts $\xi \propto c_s^{3/8}$ for flexible polyelectrolytes and $\xi \propto c_s^{1/8}$ for semiflexible polyelectrolytes. We instead recover $\xi \propto c_s^{3/4}$. Whilst we could assume this is somehow an artefact of the fitting procedure using Equation 7, this value has also been observed by Geissler *et al.* previously for the hydrodynamic correlation length extracted from dynamic light scattering.[50,51] Having found that the correlation length scales with an opposite sign and equivalent (within uncertainty) magnitude with c_s and c_p, we follow the analysis of Horkay *et al.* and can normalise the polyelectrolyte concentration by the ionic strength of the added salt (or added salt concentration for the case of monovalent salt).[49] We illustrate the results of this analysis in SI Figure **??** by plotting the fitted parameters from Equation 7 for data from both Figure 5 and 6 with a rescaled x-axis. We recover $\xi' = (10.4 \pm 2.3)(c_p/c_s)^{-0.74\pm0.05}$ Åwhich is consistent with the expected scaling for a neutral polymer in good solvent, where $\nu \simeq 0.6$. I_0 appears more sensitive to added salt concentration and is ≈ 10 times lower at high c_p/c_s values and increases with decreasing c_p/c_s.

3. Divalent Salt

To address the effect of divalent salts on the solution structure of NaCMC, we first compare the SANS profiles

from non-specifically interacting salts which exhibit H-type phase behaviour, Mg^{2+} and Na^{+}, in Figure 7 (a) and (b), respectively. Divalent ions contribute 3× the ionic strength of monovalent ions and therefore would expect equivalent molar concentrations of added divalent ions to have a proportionally greater effect on the electrostatic screening. With 0.01 M of added salt, there is a negligible difference between Mg^{2+} and Na^{+}; the correlation peak is still visible, at the same position, and scattering for $q < q^*$ appears roughly the same. This suggests Mg^{2+} binding or counterion exchange is minimal given we do not observe the expected shift in q^* to lower q values when monovalent counterions are exchanged for divalent ions.[73] Upon addition of 0.025 M Mg^{2+}, with $I \simeq 0.075$ M $> c_p$, the correlation peak and upturn at low-q completely disappear, alongside recovery of a q^{-1} dependence for $q < q^*$ (of the original correlation peak position). For a similar concentration of added Na^{+} (0.05 M), the correlation peak and low-q clustering are still evident and no q^{-1} dependence is observed, shown in Figure 7 (b) by the dotted trace.

We further compare, at low added salt concentrations, the effect of salt-type on the SANS profiles. Figure 8 (a) and (b) illustrate the effect of 0.01 M added salt at $c_p \simeq 64$ mM, with the profiles in (b) offset relative to the salt-free NaCMC. Salts which yield L-type phase behaviour (Ca^{2+}, Zn^{2+}, Ba^{2+}) appear to screen electrostatics more effectively than non-specific (Mg^{2+} and Na^{+}), yielding a shoulder on the SANS profile where the salt-free correlation peak previously appeared. The effect of further added salt (0.025 M) is illustrated in Figure 8 (c) and (d). The ionic strength contribution, or reduction in charge density upon binding,[74] of divalent salts is apparent on screening is apparent as the correlation peaks/shoulders have completely disappeared. The SANS curves sufficiently far from their respective phase boundaries appear the same (Mg^{2+}, Ca^{2+}, Zn^{2+}) whilst the most specifically interacting salt Ba^{2+}, given the phase boundary at lower added salt concentrations, exhibits excess scattering at low-q consistent with a biphasic system.

For Ca^{2+}, Zn^{2+} and Ba^{2+}, which show L-type phase behaviour, further salt addition crosses the macroscopic phase boundaries established in Figure 2. We show SANS profiles from a fixed concentration of NaCMC with added 0.1 M Ca^{2+}, 0.05 M Zn^{2+} and 0.05 M Ba^{2+} in Figure 9 (a), (b) and (c), respectively. We interpret the high-q signal as the scattering from rod-like objects with a finite cross section (black lines), using Eq. 9. The excess scattering at low which is reminiscent of that expected from randomly distributed spherical objects. We show on the plots, example fits to the Debye-Bueche model (Equation 10) and include Debye-Bueche plots as insets for $q < 0.03$ Å^{-1} (from Equation 11). Alternatively, we find acceptable fits with a polydisperse spherical form factor, which is shown in SI Figure 14. Both approaches of modelling the excess scattering confirm the presence of spherical structures with sizes in the 20-40 nm range, shown in SI Table III. The size of phase separated structures, either from the polydisperse sphere form factor or Debye-Bueche model, roughly follows the inverse of trend found for L-type phase boundaries; Ca^{2+} <Zn^{2+} <Ba^{2+}. The aggregate clusters are stable for weeks before any macrophase separation and their stability to macrophase separation also occurs in the same order as the phase boundaries.

As expected, the valency of ion is the dominant factor in screening the SANS correlation peak of NaCMC solutions, and ion specificity plays a secondary role. However, specificity is clearly crucial in emergence of the excess scattering at low-q, which we attribute to the specific binding of divalent ions, reduction in charge density of the chains and clustering. Specifically binding ions have been shown not to impart any rheological signature of intermolecular crosslinking,[75] which supports our hypothesis on the aggregate formation. Matsumoto *et al.* also provide a potential explanation for the origin of the q^{-1} feature arising upon addition of divalent salt. They suggest that divalent ions reside in an electronegative pocket near the carboxyl groups and neighbouring hydroxyl groups, off the pyranose backbone. Unlike the 'egg-box' model of complexation of Ca^{2+} from alginate, where chains laterally aggregate in cavities created by adjacent chains, the position of the divalent ion restricts the torsion angles of neighbouring pyranose groups and therefore increase the persistence length of the chain.[76] However, this explanation cannot account for the q^{-1} feature being present in excess monovalent salt, where we would expect counterions to already be condensed on the chain, irrespective of added salt concentration.

4. Analogy to changing D.S.

In Figure 10 we directly compare scattering profiles of NaCMC solutions with (a) monovalent salt addition and (b) reducing degree of substitution. Neither appears to change the position of the correlation peak but increasing salt concentration, at $c_s < c_p$, and decreasing D.S. both increase low q scattering. We can rationalize these observations by a reduction in charge density on the chain, increase the prevalance of hydrophobic associations and formation of 'pinch points' in the semidilute solution of polyelectrolyte. The physical picture of the scattering from solutions with added divalent salts is rather similar, except for the fact that cluster formation only appears upon phase separation; divalent cations are expected to complex with two carboxylate groups on the NaCMC chains causing 'kinks', *i.e.* restriction of the torsion angles between neighbouring monomers as suggested by Matsumoto.[76] Following addition of sufficient divalent ions, and a sufficient fraction bound to the NaCMC chains, the net charge on chains is reduced to near-neutral, before aggregation and phase separation take place.[52]

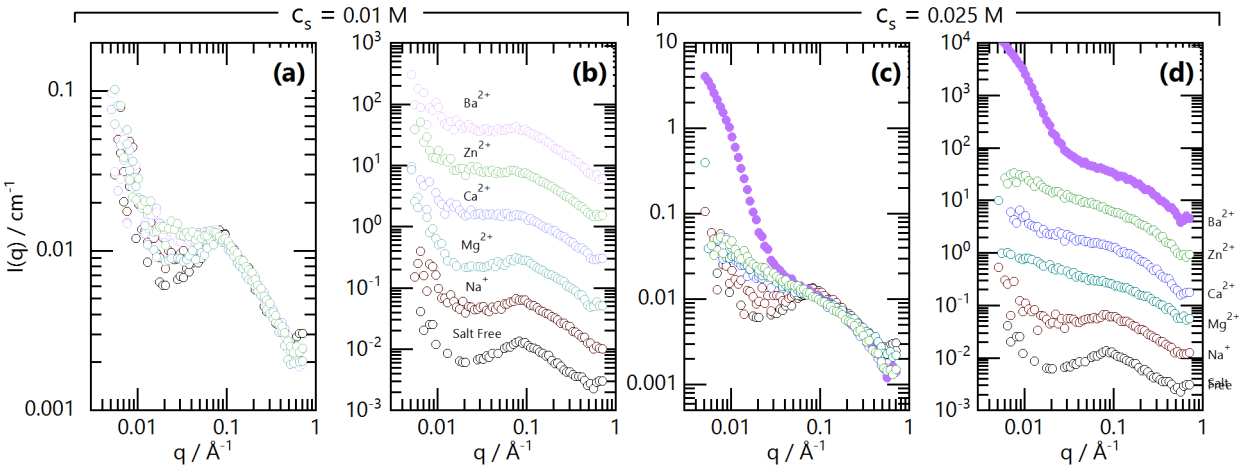

FIG. 8. (a) Coherent SANS profiles from 17.1 g L^{-1} ($\simeq$ 64 mM) NaCMC with 0.01 M added salt. Salt free NaCMC is included for reference. (b) Offset profiles from (a). Each curve is offset by 5X relative to the previous. Salt-free NaCMC is the lowest reference curve. (c) Coherent SANS profiles from 17.1 ($\simeq$ 64 mM) g L^{-1} NaCMC with 0.025 M added salt. Salt free NaCMC is included for reference. Filled symbols indicate a sample in the 2-phase region. (d) Offset profiles from (c). Each curve is offset by 5X relative to the previous. Salt-free NaCMC is the lowest reference curve.

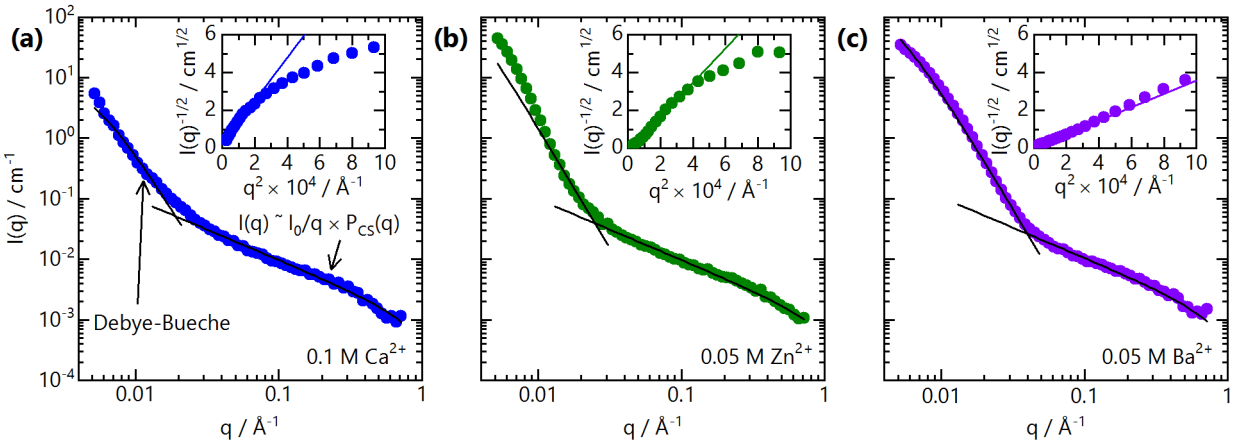

FIG. 9. 17.1 g L^{-1} ($\sim$ 64 mM) NaCMC with added (a) 0.1 M Ca^{2+} (b) 0.05 M Zn^{2+} (c) 0.05 M Ba^{2+}. Solid black lines are fits with the Debye-Bueche model (Equation 10) at low-q and Equation 9 at high-q. Insets show Debye-Bueche plots with solid lines linear fits to the transformed data.

V. CONCLUSIONS

In summary, we have shown that NaCMC exhibits phase behaviour in the presence of added salt which is characteristic of the valency and specific binding of the oppositely charged ion to the polyelectrolyte. Na^+ and Mg^{2+} yield H-type phase behaviour, typical of non-specific electrostatic interactions, whilst Ca^{2+}, Zn^{2+} and Ba^{2+} yield a mixed-L type phase behaviour. We established phase boundaries with added salt and found the critical salt concentration required to induced turbidity in NaCMC solutions to be invariant to NaCMC concentration for $c_p <$ a critical value $c_p^* \lesssim 10$ mM and then proportional to c_p for $c \gtrsim c_p^*$ with slope c_s/c_p. The value of the low c_p plateau ($c_{s,0}$), c_p^* and c_s/c_p all appeared to be correlated to the ion type and we propose this is related to the relative ion binding strengths of each ion to the NaCMC carboxylate function groups.

We then investigated the structure of NaCMC solutions in the presence of monovalent and divalent salts over a wide concentration range (0 - 2 M added salt) by SANS. Firstly, upon addition of monovalent salt, NaCl, at a fixed c_p ($\sim$ 64 mM) we find that the correlation peak remains apparent at a fixed position q^* for $c_s < c_p$ and disappears for $c_s > c_p$, associated with screening. Also for $c_s > c_p$ a q^{-1} dependence emerges in the SANS profile, which appears to increase in q-range, eventually covering almost 3 decades in q, with increasing c_s. In the absence of rigorous models for the scattering from semiflexible semidilute polymer solutions, we follow the

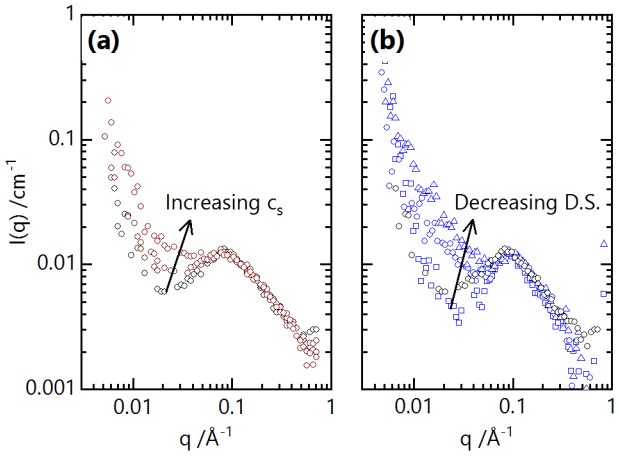

FIG. 10. (a) Coherent SANS profiles for 17.1 g L^{-1} NaCMC and added NaCl from 0 - 0.05 M. (b) Comparison with of salt-free NaCMC of varying D.S.. Literature data taken from Ref. [55]. (○) This work - 17.1 g L^{-1} D.S. = 1.3 (□) 20 g L^{-1} D.S. = 1.2 (○) 20 g L^{-1} D.S. = 0.8 and (△) 16 g L^{-1} D.S. = 0.7.

descriptive approach of Horkay *et al.* and fit Equation 7 to SANS data from solutions of NaCMC with a varying c_s and at a fixed excess c_s (2 M) with varying c_p. The model is found to be adequate for sufficiently screened polyelectrolytes, where the correlation peak is absent *i.e.* for $c_s \geq c_p$. We find the fitting procedure to be self-consistent, and scaling of both the fitted prefactor I_0 and correlation length ξ' recover the asymptotic limit of the model. We find the scaling of ξ' with c_p is indicative of a neutral flexible polymer in good solvent and that by scaling by the ionic strength of the added salt, this behaviour is general for any concentration of excess salt. This suggests that non-specifically interacting salts solely screen electrostatic interactions between neighbouring chains on small length scales. The semiflexible chains retains their rigidity (rod-like behaviour) for $q > 1/\xi$' and adopt a self-avoiding random walk for $q < 1/\xi$'.

Upon addition of divalent salts, the 3× greater contribution to the ionic strength causes screening of the correlation peak in the SANS data at much lower concentrations ($c_s < 1/2c_p$). Non-specifically interacting ions (viz. Mg^{2+}) are qualitatively less effective than specifically interacting ions (Ca^{2+}, Zn^{2+} and Ba^{2+}). In this case, the effects are subtle and secondary to the effect of the ionic strength. For compositions which reside in the 2-phase region, the mid-high q scattering appears unchanged whilst excess scattering is prevalent at low-q. We interpret the low-q data in terms of a polydisperse spherical form factor or, alternatively, with the Debye-Bueche model, which maps the spatial correlations of heterogeneous 2-phase systems. Both approaches resolve $\approx 20-40$ nm sized objects which impart the turbidity observed optically. We suggest that phase separation arises from multiple chain aggregates, which associate as the charge density of the chain reduces to near neutral upon divalent ion binding and liken both the effects of monovalent and divalent ions to that of reducing the charge density of the chain by changing the D.S. of NaCMC. We schematically outline our main conclusions in Figure 11.

ACKNOWLEDGEMENTS

We acknowledge the Engineering and Physical Sciences Research Council (EPSRC, UK) and Procter & Gamble for funding. We gratefully acknowledge the Science and Technology Facilities Council (STFC) for access to neutron beamtime on SANS2D at ISIS and Nikul Khunti and the B21 Beamline at Diamond Light Source for running the SAXS measurements as part of their mail-in service.

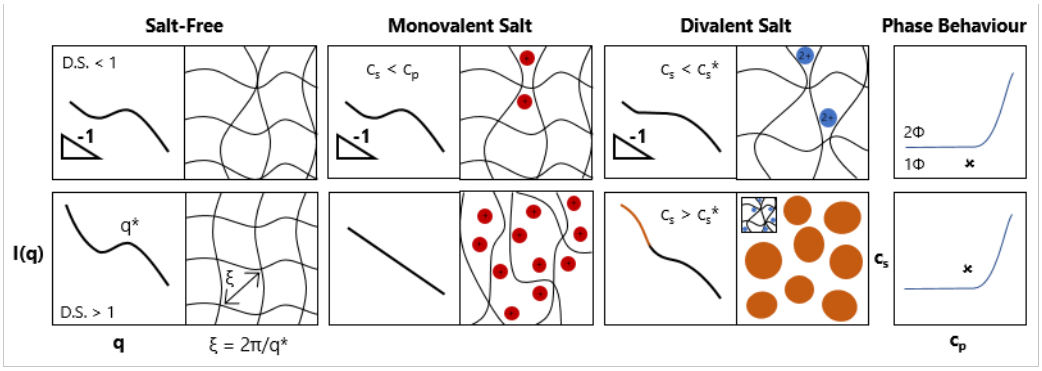

FIG. 11. Physical interpretation of semidilute NaCMC solutions with varying D.S. and added salts, monovalent or divalent. In each column, boxes on the left are the SANS profile and boxes on the right are the physical interpretation of the semidilute solution. Salt free solutions exhibit a correlation peak, where $\xi = 2\pi/q^*$ and q^* is the peak position, as well as clustering at low q, which increases with decreasing D.S. In monovalent salts, at low concentrations the solution appears similar to low D.S. salt-free solutions. In excess monovalent salt, correlations are screened and a rod-like (q^{-1}) structure is observed over the whole q-range in SANS. Upon divalent salt addition up to the phase boundary ($c_s < c_s^*$), complexation leads to formation of 'pinch points' alongside stronger electrostatic screening (relative to monovalent salt) and results in disappearance of the correlation peak and a q^{-1} dependence appear. Upon addition of salt past the phase boundary ($c_s > c_s^*$), phase separation ensues creating 20-40 nm clusters and a resulting excess scattering at low q in the SANS profile coexisting with the molecularly soluble and highly screened chains.

VI. MATERIALS AND METHODS

A. Sample Preparation

A NaCMC sample with nominal $M_w = 2.5 \times 10^5$ g/mol and D.S. = 1.15-1.35 was purchased from Sigma-Aldrich. The molar mass and degree of substitution were evaluated in an earlier contribution to be $M_w \simeq 2.1 \times 10^5$ g/mol and D.S. $\simeq 1.3$. Deionised (DI) water was obtained from a Milli-Q source. Heavy water (99.9% D, Sigma Aldrich), sodium chloride (NaCl, Fluka puriss. p.a. 99.5%), calcium chloride ($CaCl_2$, VWR 2-5mm granules 94%), barium chloride ($BaCl_2$, Sigma Aldrich 99.999%), zinc chloride ($ZnCl_2$, puriss. p.a., ACS reagent, reag. ISO, reag. Ph. Eur., 98%), magnesium chloride hexahydrate ($MgCl_2.6H_2O$, VWR ACS, Reag. Ph. Eur. 99.0-101.0 %), iron (II) chloride ($FeCl_2$, Sigma Aldrich anhydrous 99.99%) were used without further purification. Solutions were prepared by dissolving the NaCMC in either DI water or D_2O, with the aid of a roller mixer, followed by addition of the corresponding salt and further homogenisation on the roller mixer. NaCMC concentrations are reported in mass (of polymer) per litre of solvent or in moles of monomer per litre of solvent. The hygroscopicity of NaCMC and residual water content is accounted for in the concentrations reported herein. For the NaCMC studied, here TGA measurements resolved a bulk water content of $9.6 \pm 2.8\%$, whilst SANS measurements resolved $\simeq 15 \pm 4\%$ from the incoherent background assuming a polymer incoherent scattering contribution of $S_{inc,NaCMC} = 0.60 \pm 0.05 \text{cm}^{-1}$

B. Small Angle Neutron Scattering Measurements

Time of flight SANS experiments were undertaken at the SANS2D beamline (ISIS, STFC, Harwell, UK) with detector distances of 2.4 and 4 m, yielding a q range of 0.005 - 0.97 Å. Data were truncated at 0.72 Å. Quartz cells (Hellma) of 5 mm path length were used for all samples. MANTID was used to reduce the data, according to standard procedures, and to merge the scattering profiles from both detectors.[77]

C. Small Angle X-Ray Scattering Measurements

Small angle X-ray scattering (SAXS) measurements were performed on the B21 beamline at Diamond Light Source, UK. Samples were measured in batch mode using an EMBL Arinax sample handling robot which dispensed prepared samples into a temperature-controlled quartz glass capillary. The X-ray beam (12.4 keV / 0.99 Å) was scattered by the sample and detected on a Pilatus 2M 2D detector at 4.014m from the sample position yielding a q-range of $0.005 < q < 0.4$ Å^{-1}. The intensity is reported in arbitrary units and the detector pixels calibrated with Silver Behenate (AgBeH) to yield accurate q assignments. Data reported have been corrected for the solvent and cell scattering.

D. Phase Behaviour

The phase boundaries were determined by assessing the turbidity of the samples ($\simeq$ 5 mL in a glass vial) by

eye. All data were measured at room temperature (25 °C and 40-50 % relative humidity).

E. Partial Molar Volume Determination

Density measurements were performed in triplicate, for each sample, on an Anton Paar DMA™1001 Density Meter at 25.00 ± 0.01 °C. The oscillating tube was calibrated with air and DI water at 20 °C prior to each set of measurements. The measuremental precision was 1 $\times 10^{-5}$ g cm^{-3} and repeat measurements gave, on average, differences of $\simeq 1 \times 10^{-5}$ g cm^{-3} which suggests a similar level of accuracy. Partial molar volume ($\bar{V}$) was calculated via the same approach as Tondre, Zana and Wandrey.[78–80]

VII. REFERENCES

[1] C. Clasen and W.-M. Kulicke, "Determination of viscoelastic and rheo-optical material functions of water-soluble cellulose derivatives," *Prog. Polym. Sci.*, vol. 26, no. 9, pp. 1839 – 1919, 2001.

[2] Z. Cai, J. Wu, B. Du, and H. Zhang, "Impact of distribution of carboxymethyl substituents in the stabilizer of carboxymethyl cellulose on the stability of acidified milk drinks," *Food hydrocolloids*, vol. 76, pp. 150–157, 2018.

[3] O. Yuliarti, K. H. Mei, Z. K. X. Ting, and K. Y. Yi, "Influence of combination carboxymethylcellulose and pectin on the stability of acidified milk drinks," *Food hydrocolloids*, vol. 89, pp. 216–223, 2019.

[4] J. Wu, J. Liu, Q. Dai, and H. Zhang, "The stabilisation of acidified whole milk drinks by carboxymethylcellulose," *International dairy journal*, vol. 28, no. 1, pp. 40–42, 2013.

[5] C. G. Lopez and W. Richtering, "Influence of divalent counterions on the solution rheology and supramolecular aggregation of carboxymethyl cellulose," *Cellulose*, vol. 26, no. 3, pp. 1517–1534, 2019.

[6] E. Turkoz, A. Perazzo, C. B. Arnold, and H. A. Stone, "Salt type and concentration affect the viscoelasticity of polyelectrolyte solutions," *Applied Physics Letters*, vol. 112, no. 20, p. 203701, 2018.

[7] A. García, M. Culebras, M. N. Collins, and J. J. Leahy, "Stability and rheological study of sodium carboxymethyl cellulose and alginate suspensions as binders for lithium ion batteries," *Journal of Applied Polymer Science*, vol. 135, no. 17, p. 46217, 2018.

[8] R. J. Nap and I. Szleifer, "Effect of calcium ions on the interactions between surfaces end-grafted with weak polyelectrolytes," *The Journal of chemical physics*, vol. 149, no. 16, p. 163309, 2018.

[9] C. G. Lopez, S. E. Rogers, R. H. Colby, P. Graham, and J. T. Cabral, "Structure of sodium carboxymethyl cellulose aqueous solutions: A sans and rheology study," *Journal of Polymer Science Part B: Polymer Physics*, vol. 53, no. 7, pp. 492–501, 2015.

[10] E. Arinaitwe and M. Pawlik, "Dilute solution properties of carboxymethyl celluloses of various molecular weights and degrees of substitution," *Carbohydr Polym*, vol. 99, no. Supplement C, pp. 423–31, 2014.

[11] M. Karataş and N. Arslan, "Flow behaviours of cellulose and carboxymethyl cellulose from grapefruit peel," *Food hydrocolloids*, vol. 58, pp. 235–245, 2016.

[12] Note also that approximately 50% of the counter-ions are condensed into the chain.

[13] M. Rubinstein and R. H. Colby, *Polymer Physics*. Oxford, 2003.

[14] R. H. Colby, "Structure and linear viscoelasticity of flexible polymer solutions: comparison of polyelectrolyte and neutral polymer solutions," *Rheol. Acta*, vol. 49, no. 5, pp. 425–442, 2010.

[15] C. G. Lopez, R. H. Colby, P. Graham, and J. T. Cabral, "Viscosity and scaling of semiflexible polyelectrolyte nacmc in aqueous salt solutions," *Macromolecules*, vol. 50, no. 1, pp. 332–338, 2016.

[16] B. Hammouda, D. L. Ho, and S. Kline, "Insight into clustering in poly(ethylene oxide) solutions," *Macromolecules*, vol. 37, no. 18, pp. 6932–6937, 2004.

[17] P. Debye and A. M. Bueche, "Scattering by an inhomogeneous solid," *Journal of Applied Physics*, vol. 20, no. 6, pp. 518–525, 1949.

[18] P. Debye, H. R. Anderson, and H. Brumberger, "Scattering by an inhomogeneous solid. ii. the correlation function and its application," *Journal of Applied Physics*, vol. 28, no. 6, pp. 679–683, 1957.

[19] A. Ikegami and N. Imai, "Precipitation of polyelectrolytes by salts," *Journal of Polymer Science*, vol. 56, no. 163, pp. 133–152, 1962.

[20] M. Hansch, B. Hämisch, R. Schweins, S. Prévost, and K. Huber, "Liquid-liquid phase separation in dilute solutions of poly (styrene sulfonate) with multivalent cations: Phase diagrams,

chain morphology, and impact of temperature," *The Journal of chemical physics*, vol. 148, no. 1, p. 014901, 2018.
[21]M. Hansch, H. P. Kaub, S. Deck, N. Carl, and K. Huber, "Reaction enthalpy from the binding of multivalent cations to anionic polyelectrolytes in dilute solutions," *The Journal of chemical physics*, vol. 148, no. 11, p. 114906, 2018.
[22]F. T. Wall and J. W. Drenan, "Gelation of polyacrylic acid by divalent cations," *Journal of Polymer Science*, vol. 7, no. 1, pp. 83–88, 1951.
[23]I. Michaeli, "Ion binding and the formation of insoluble polymethacrylic salts," *Journal of Polymer Science*, vol. 48, no. 150, pp. 291–299, 1960.
[24]K. A. Narh and A. Keller, "Precipitation effects in polyelectrolytes on addition of salts," *Journal of Polymer Science Part B-Polymer Physics*, vol. 31, no. 2, pp. 231–234, 1993.
[25]N. Volk, D. Vollmer, M. Schmidt, W. Oppermann, and K. Huber, *Conformation and Phase Diagrams of Flexible Polyelectrolytes*, pp. 29–65. Berlin, Heidelberg: Springer Berlin Heidelberg, 2004.
[26]R. Schweins, G. Goerigk, and K. Huber, "Shrinking of anionic polyacrylate coils induced by ca2+, sr2+ and ba2+: a combined light scattering and asaxs study," *Eur Phys J E Soft Matter*, vol. 21, no. 2, pp. 99–110, 2006.
[27]S. Lages, R. Schweins, and K. Huber, "Temperature-induced collapse of alkaline earth cation-polyacrylate anion complexes," *J Phys Chem B*, vol. 111, no. 35, pp. 10431–7, 2007.
[28]V. Prabhu, M. Muthukumar, G. Wignall, and Y. Melnichenko, "Dimensions of polyelectrolyte chains and concentration fluctuations in semidilute solutions of sodium–poly (styrene sulfonate) as measured by small-angle neutron scattering," *Polymer*, vol. 42, no. 21, pp. 8935–8946, 2001.
[29]V. Prabhu, M. Muthukumar, G. D. Wignall, and Y. B. Melnichenko, "Polyelectrolyte chain dimensions and concentration fluctuations near phase boundaries," *The Journal of chemical physics*, vol. 119, no. 7, pp. 4085–4098, 2003.
[30]M. A. V. Axelos, M. M. Mestdagh, and J. Francois, "Phase diagrams of aqueous solutions of polycarboxylates in the presence of divalent cations," *Macromolecules*, vol. 27, no. 22, pp. 6594–6602, 1994.
[31]J. Franois, N. D. Truong, G. Medjahdi, and M. M. Mestdagh, "Aqueous solutions of acrylamide-acrylic acid copolymers: stability in the presence of alkalinoearth cations," *Polymer*, vol. 38, no. 25, pp. 6115–6127, 1997.
[32]I. Sabbagh and M. Delsanti, "Solubility of highly charged anionic polyelectrolytes in presence of multivalent cations: Specific interaction effect," *The European Physical Journal E*, vol. 1, no. 1, pp. 75–86, 2000.
[33]C. G. Sinn, R. Dimova, and M. Antonietti, "Isothermal titration calorimetry of the polyelectrolyte/water interaction and binding of ca2+: Effects determining the quality of polymeric scale inhibitors," *Macromolecules*, vol. 37, no. 9, pp. 3444–3450, 2004.
[34]M. Rinaudo and M. Milas, "Interaction of monovalent and divalent counterions with some carboxylic polysaccharides," *Journal of Polymer Science Part a-Polymer Chemistry*, vol. 12, no. 9, pp. 2073–2081, 1974.
[35]T. Matsumoto and H. Zenkoh, "A new molecular model for complexation between carboxymethylcellulose and alkalineearth metal ions in aqueous systems," *Food Hydrocolloids*, vol. 6, no. 4, pp. 379–386, 1992.
[36]A. Haug and O. Smidsrd, "Selectivity of some anionic polymers for divalent metal ions," *Acta Chemica Scandinavica*, vol. 24, pp. 843–854, 1970.
[37]K. Kamide, M. Saito, and H. Suzuki, "Persistence length of cellulose and cellulose derivatives in solution," *Makromolekulare Chemie-Rapid Communications*, vol. 4, no. 1, pp. 33–39, 1983.
[38]C. W. Hoogendam, A. de Keizer, M. A. C. Stuart, B. H. Bijsterbosch, J. A. M. Smit, J. A. P. P. van Dijk, P. M. van der Horst, and J. C. Batelaan, "Persistence length of carboxymethyl cellulose as evaluated from size exclusion chromatography and potentiometric titrations," *Macromolecules*, vol. 31, no. 18, pp. 6297–6309, 1998.
[39]P. Sharp and V. A. Bloomfield, "Light scattering from wormlike chains with excluded volume effects," *Biopolymers*, vol. 6, no. 8, pp. 1201–11, 1968.
[40]J. des Cloizeaux, "Form factor of an infinite kratky-porod chain," *Macromolecules*, vol. 6, no. 3, pp. 403–407, 1973.
[41]J. S. Pedersen and P. Schurtenberger, "Scattering functions of semiflexible polymers with and without excluded volume effects," *Macromolecules*, vol. 29, no. 23, pp. 7602–7612, 1996.
[42]B. McCulloch, V. Ho, M. Hoarfrost, C. Stanley, C. Do, W. T. Heller, and R. A. Segalman, "Polymer chain shape of poly(3-alkylthiophenes) in solution using small-angle neutron scattering," *Macromolecules*, vol. 46, no. 5, pp. 1899–1907, 2013.
[43]M. Yang, W. Zhao, S. Wang, C. Yu, S. Singh, B. Simmons, and G. Cheng, "Dimethyl sulfoxide assisted dissolution of cellulose in 1-ethyl-3-methylimidazoium acetate: small angle neutron scattering and rheological studies," *Cellulose*, vol. 26, no. 4, pp. 2243–2253, 2019.
[44]E. Dubois and F. Bou, "Conformation of poly(styrenesulfonate) polyions in the presence of multivalent ions: small-angle neutron scattering experiments," *Macromolecules*, vol. 34, no. 11, pp. 3684–3697, 2001.
[45]M. Spiteri, "Thesis, université orsay - paris-sud, 1997."
[46]R. S. Koene and M. Mandel, "Scaling relations for aqueous polyelectrolyte-salt solutions. 1. quasi-elastic light scattering as a function of polyelectrolyte concentration and molar mass," *Macromolecules*, vol. 16, no. 2, pp. 220–227, 1983.
[47]R. S. Koene, T. Nicolai, and M. Mandel, "Scaling relations for aqueous polyelectrolyte-salt solutions. 2. quasi-elastic light scattering as a function of polyelectrolyte concentration and salt concentration," *Macromolecules*, vol. 16, no. 2, pp. 227–231, 1983.
[48]F. Horkay, P. J. Basser, A. M. Hecht, and E. Geissler, "Ionic effects in semi-dilute biopolymer solutions: A small angle scattering study," *J Chem Phys*, vol. 149, no. 16, p. 163312, 2018.
[49]F. Horkay, P. J. Basser, A.-M. Hecht, and E. Geissler, "Chondroitin sulfate in solution: Effects of mono- and divalent salts," *Macromolecules*, vol. 45, no. 6, pp. 2882–2890, 2012.
[50]E. Geissler, A. M. Hecht, and F. Horkay, "Scaling equations for a biopolymer in salt solution," *Phys Rev Lett*, vol. 99, no. 26, p. 267801, 2007.
[51]E. Geissler, A. M. Hecht, and F. Horkay, "Scaling behaviour of hyaluronic acid in solution with mono- and divalent ions," *Macromol Symp*, vol. 291-292, no. 1, pp. 362–370, 2010.
[52]K. Huber, "Calcium-induced shrinking of polyacrylate chains in aqueous solution," *The Journal of Physical Chemistry*, vol. 97, no. 38, pp. 9825–9830, 1993.
[53]K. Kassapidou, W. Jesse, M. E. Kuil, A. Lapp, S. Egelhaaf, and J. R. C. van der Maarel, "Structure and charge distribution in dna and poly(styrenesulfonate) aqueous solutions," *Macromolecules*, vol. 30, no. 9, pp. 2671–2684, 1997.
[54]A. V. Dobrynin, R. H. Colby, and M. Rubinstein, "Scaling theory of polyelectrolyte solutions," *Macromolecules*, vol. 28, no. 6, pp. 1859–1871, 1995.
[55]C. G. Lopez, R. H. Colby, and J. T. Cabral, "Electrostatic and hydrophobic interactions in nacmc aqueous solutions: Effect of degree of substitution," *Macromolecules*, vol. 51, no. 8, pp. 3165–3175, 2018.
[56]M. Nierlich, F. Boue, A. Lapp, and R. Oberthur, "Characteristic lengths and the structure of salt free polyelectrolyte solutions - a small-angle neutron-scattering study," *Colloid and Polymer Science*, vol. 263, no. 12, pp. 955–964, 1985.
[57]R. Borsali, M. Rinaudo, and L. Noirez, "Light-scattering and small-angle neutron-scattering from polyelectrolyte solutions - the succinoglycan," *Macromolecules*, vol. 28, no. 4, pp. 1085–1088, 1995.
[58]R. Borsali, H. Nguyen, and R. Pecora, "Small-angle neutron scattering and dynamic light scattering from a polyelectrolyte solution: Dna," *Macromolecules*, vol. 31, no. 5, pp. 1548–1555, 1998.
[59]A. Patkowski, E. Gulari, and B. Chu, "Long range trnatrna electrostatic interactions in saltfree and lowsalt trna solutions," *The Journal of Chemical Physics*, vol. 73, no. 9, pp. 4178–4184, 1980.

[60]L. Wang and V. A. Bloomfield, "Small-angle x-ray scattering of semidilute rodlike dna solutions: polyelectrolyte behavior," *Macromolecules*, vol. 24, no. 21, pp. 5791–5795, 1991.
[61]W. Essafi, F. Lafuma, and C. E. Williams, *Structure of Polyelectrolyte Solutions at Intermediate Charge Densities*, vol. 548 of *ACS Symposium Series*, book section 21, pp. 278–286. American Chemical Society, 1993.
[62]W. Essafi, F. Lafuma, and C. Williams *The European Physical Journal B*.
[63]K. Nishida, K. Kaji, T. Kanaya, and T. Shibano, "Added salt effect on the intermolecular correlation in flexible polyelectrolyte solutions: small-angle scattering study," *Macromolecules*, vol. 35, no. 10, pp. 4084–4089, 2002.
[64]M. Nierlich, C. Williams, F. Boue, J. Cotton, M. Daoud, B. Famoux, G. Jannink, C. Picot, M. Moan, C. Wolff, M. Rinaudo, and P. de Gennes, "Small angle neutron scattering by semidilute solutions of polyelectrolyte," *Journal de Physique*, vol. 40, no. 7, pp. 701–704, 1979.
[65]I. Morfin, W. F. Reed, M. Rinaudo, and R. Borsali, "Further evidence of liquid-like correlations in polyelectrolyte solutions," *Journal De Physique Ii*, vol. 4, no. 6, pp. 1001–1019, 1994.
[66]D. Truzzolillo, F. Bordi, C. Cametti, and S. Sennato, "Counterion condensation of differently flexible polyelectrolytes in aqueous solutions in the dilute and semidilute regime," *Phys Rev E Stat Nonlin Soft Matter Phys*, vol. 79, no. 1 Pt 1, p. 011804, 2009.
[67]K. Hayashi, K. Tsutsumi, T. Norisuye, and A. Teramoto, "Electrostatic contributions to chain stiffness and excluded-volume effects in sodium hyaluronate solutions," *Polymer Journal*, vol. 28, no. 10, pp. 922–928, 1996.
[68]D. M. Rein, R. Khalfin, N. Szekely, and Y. Cohen, "True molecular solutions of natural cellulose in the binary ionic liquid-containing solvent mixtures," *Carbohydrate Polymers*, vol. 112, pp. 125–133, 2014.
[69]T. Kawaguchi, "Application of isoscattering points to the analysis of globular solute structures," *Crystallography Reviews*, vol. 10, no. 3, pp. 233–246, 2004.
[70]T. Shimada, M. Doi, and K. Okano, "Concentration fluctuation of stiff polymers. i. static structure factor," *The Journal of Chemical Physics*, vol. 88, no. 4, pp. 2815–2821, 1988.
[71]T. Odijk, "Possible scaling relations for semidilute polyelectrolyte solutions," *Macromolecules*, vol. 12, no. 4, pp. 688–693, 1979.
[72]J. F. Joanny and P. Pincus, "Electrolyte and polyelectrolyte solutions: limitations of scaling laws, osmotic compressibility and thermoelectric power," *Polymer*, vol. 21, no. 3, pp. 274–278, 1980.
[73]Y. B. Zhang, J. F. Douglas, B. D. Ermi, and E. J. Amis, "Influence of counterion valency on the scattering properties of highly charged polyelectrolyte solutions," *Journal of Chemical Physics*, vol. 114, no. 7, pp. 3299–3313, 2001.
[74]G. S. Manning, "Limiting laws and counterion condensation in polyelectrolyte solutions i. colligative properties," *The Journal of Chemical Physics*, vol. 51, no. 3, pp. 924–933, 1969.
[75]T. Matsumoto and D. Ito, "Viscoelastic and nuclear-magnetic-resonance studies on molecular mobility of carboxymethylcellulose calcium complex in concentrated aqueous systems," *Journal of the Chemical Society-Faraday Transactions*, vol. 86, no. 5, pp. 829–832, 1990.
[76]T. Matsumoto and H. Zenkoh, "A new molecular model for complexation between carboxymethylcellulose and alkalineearth metal ions in aqueous systems," *Food Hydrocolloids*, vol. 6, no. 4, pp. 379–386, 1992.
[77]O. Arnold, J. C. Bilheux, J. M. Borreguero, A. Buts, S. I. Campbell, L. Chapon, M. Doucet, N. Draper, R. Ferraz Leal, M. A. Gigg, V. E. Lynch, A. Markvardsen, D. J. Mikkelson, R. L. Mikkelson, R. Miller, K. Palmen, P. Parker, G. Passos, T. G. Perring, P. F. Peterson, S. Ren, M. A. Reuter, A. T. Savici, J. W. Taylor, R. J. Taylor, R. Tolchenov, W. Zhou, and J. Zikovsky, "Mantiddata analysis and visualization package for neutron scattering andsr experiments," *Nuclear Instruments and Methods in Physics Research Section A: Accelerators, Spectrometers, Detectors and Associated Equipment*, vol. 764, pp. 156–166, 2014.
[78]C. Tondre and R. Zana, "Apparent molal volumes of polyelectrolytes in aqueous solutions," *The Journal of Physical Chemistry*, vol. 76, no. 23, pp. 3451–3459, 1972.
[79]R. Zana, "Partial molal volumes of polymers in aqueous solutions from partial molal volume group contributions," *Journal of Polymer Science: Polymer Physics Edition*, vol. 18, no. 1, pp. 121–126, 1980.
[80]C. Wandrey, A. Bartkowiak, and D. Hunkeler, "Partial molar and specific volumes of polyelectrolytes: comparison of experimental and predicted values in salt-free solutions," *Langmuir*, vol. 15, no. 12, pp. 4062–4068, 1999.
[81]F. J. Millero, "Molal volumes of electrolytes," *Chemical Reviews*, vol. 71, no. 2, pp. 147–176, 1971.
[82]S. Koda, S. Hasegawa, M. Mikuriya, F. Kawaizumi, and H. Nomura, "Hydration of carboxymethyl cellulose and carboxymethyl dextran," *Polymer*, vol. 29, no. 11, pp. 2100–2104, 1988.

VIII. SUPPLEMENTARY INFORMATION

A. Scattering Contrasts

Table II details partial molecular volumes, scattering lengths and calculated contrasts from Equation **??** for species involved in this study.

B. Modelling Polyelectrolyte Phase Behaviour

Axelos *et al.* introduced a mass balance model to describe the critical divalent salt concentration required to precipitate polyelectrolytes as a sum of free and bound divalent ions,[30] which in its simplest form is expressed in Equation 12. Equation 13 gives the concentration of divalent ions bound to the polyelectrolyte, which can be simply described by the fraction bound and the concentration of polyelectrolyte charged groups and adjusted for valency of the salt. The free ion contribution, given in Equation 14 is derived from the equilibrium between divalent ions and can qualitatively describe the critical salt concentration as a function of polymer concentration, fraction of bound ions (f^*) complexed by the polyelectrolyte and the binding constant of the polyelectrolyte-salt complex (K_B), illustrated in Equation 15.

$$[M^{2+}] = [M^{2+}]_{bound} + [M^{2+}]_{free} \tag{12}$$

$$[M^{2+}]_{bound} = \frac{f^*[COO^-]}{2} \tag{13}$$

$$[M^{2+}]_{free} = \frac{f^*}{2K_B[COO^-](1-f^*)^2} \tag{14}$$

$$K_B = \frac{[(COO)_2M]}{[COO^-]^2[M^{2+}]} \tag{15}$$

In Figure 12 we show fits of the above model to our data in main paper Figure 2, which are illustrative of a mixed L-type phase behaviour. With only two fitting parameters, f^* and K_B, the model can qualitatively describe the Ba^{2+} and Zn^{2+} data. However, we find disagreement between the fraction of bound ions with reports from Matsumoto *et al.* who found that $\sim$ 92 % of Ba cations are bound to NaCMC.[35] The model also fails to describe data with a higher $[M^{2+}]_0$, such as here for the Ca^{2+} data. Counterion condensation and ionic strength effects on the screening length are neglected in the model. Equally, charged groups are considered isolated and therefore binding of a divalent ion to two groups on the same chain or between chains is indistinguishable. Therefore it may not accurately predict the data. It also predicts an upturn at low concentrations of polyelectrolyte, where the the free ion term dominates. Our experimental approach of resolving the turbidity optical cannot discern a polyelectrolyte independent phase boundary and an upturn, which has also been previously observed for poly(acrylate) and poly(vinyl sulfonate) with calcium ions.[32]

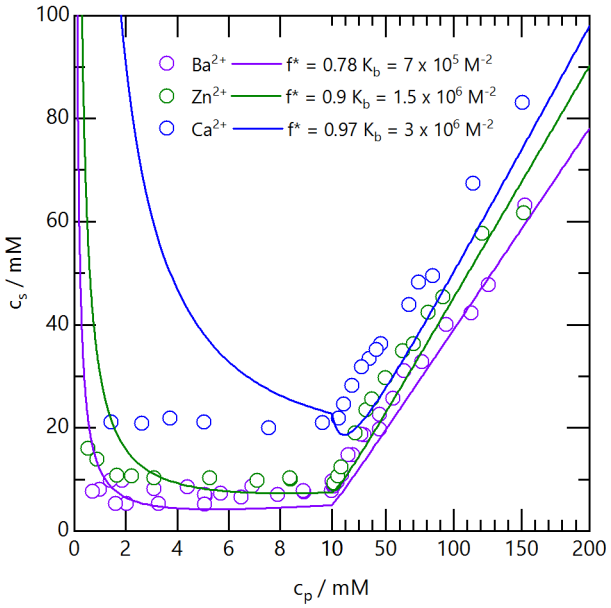

FIG. 12. Comparison of experimental phase behaviour with the model from Axelos *et al.* in Ref. [30].

C. Partial Molar Volume of Polyelectrolytes

The partial specific volume $\bar{v}$ (in mL g^{-1}), the change in total volume per unit of solute mass added at constant temperature and pressure $(\frac{\partial V}{\partial m})_{T,p}$ can be related to the partial molar volume $\bar{V}$ (in mL mol^{-1}) by substitution of mass added for moles through:

$$\bar{v} = \frac{\bar{V}}{m} \tag{16}$$

where, as in the main text, m is the molecular weight of the solute. Experimentally, both quantities are calculated from density measurements with varying concentrations of solute(s). For NaCMC, we measure the density as a function of both polyelectrolyte concentration (4 $\times 10^{-3}$ - 2.5 $\times 10^{-2}$ g mL^{-1}) and added monovalent salt concentration (0 - 2 M), as shown in Figure 13 (a). The density increases with both NaCMC concentration and NaCl concentration. The pure solution density and the partial specific volume (assuming no NaCMC concentration dependence) can be recovered through the following relation, which is fitted to the data.

$$\rho = \rho_0 + (1 - \bar{v_s}\rho_0)c \tag{17}$$

Following conversion to a partial molar volume, using Equation 16, this approach consistently overestimates the partial molar volume. Instead, we opt to explicitly calculate the partial molar volume for each composition/measured density using

Species (i)	Partial molar volume ($\bar{V}_i$) / mL mol^{-1}	Scattering length (b) / fm	Scattering length contrast ($\bar{b}_i$) / fm
H_2O	18.1	-1.68	-
D_2O	18.1	19.1	-
Na^+	-1.21[a]	3.63	4.92
Cl^-	17.8[a]	9.58	-9.31
NaCl	16.6	13.2	-4.40
CMC^-	132[b]	59.0	-81.2
NaCMC	134[c]	63.7	-77.8
Mg^{2+}	-21.2[a]	5.38	27.8
Ca^{2+}	-17.9[a]	4.70	23.6
Zn^{2+}	-21.6[a]	5.68	26.8
Ba^{2+}	-12.5[a]	5.07	18.3
$Mg_{1/2}CMC$	122[b]	61.7	-69.4
$Ca_{1/2}CMC$	123[b]	61.4	-67.3
$Zn_{1/2}CMC$	122[b]	61.8	-72.1
$Ba_{1/2}CMC$	126[b]	61.5	-66.9

TABLE II. Table of partial molar volumes and constrast factors for species involved in SANS experiments. [a] Partial molar volumes for ions taken from Table 3 in Ref. [81] at 25°C. [b] Partial molar volume calculated from the sum or difference between literature and measured values. [c] Partial molar volume for NaCMC calculated from the density measurements present below in Figure 13.

$$\bar{v} = \frac{M}{\rho_0} - \frac{10^3}{c}\left(\frac{\rho}{\rho_0} - 1\right) \tag{18}$$

which is illustrated in Figure 13 (b). By taking an average and standard deviation over concentration invariant ranges we can determine, with some accuracy, the partial molar volume ($\bar{V}$) of NaCMC in NaCl salt solutions. These values, consistent with previous literature for salt-free NaCMC with D.S. = 1.3,[82] are plotted in Figure 13 (c). The partial molar volume increases with salt concentration.

D. Size of Aggregate Structures for NaCMC with Divalent Ions

Table III shows the sizes of aggregates observed by SANS for NaCMC in the presence of divalent ions, past the macroscopic phase boundary. Sizes are obtained from the low-q excess scattering by two approaches: fitting a polydisperse spherical form factor, shown in Figure 14, or by transforming the low q data using the Debye-Bueche model to a linearised form from which a correlation length can be extracted.

E. Universal Behaviour of Monovalent Salt on ξ'

All SANS data with excess monovalent salt (> 0.25 M) can be rescaled by normalising the polymer concentration c_p by the added salt concentration c_s. The effect on the Horkay model (Equation 7) prefactor (I_0) and correlation length (ξ') are shown in Figure 15 (a) and (b), respectively. The I_0 values do not collapse as they are largely set by the compressibility of the solution, which is predominantly a function of c_s. The ξ' values do all collapse onto the same master curve, suggesting that sufficient screening of short-range repulsive interactions can cause chains to follow self-avoiding random walk statistics for $q < 1/\xi$'.

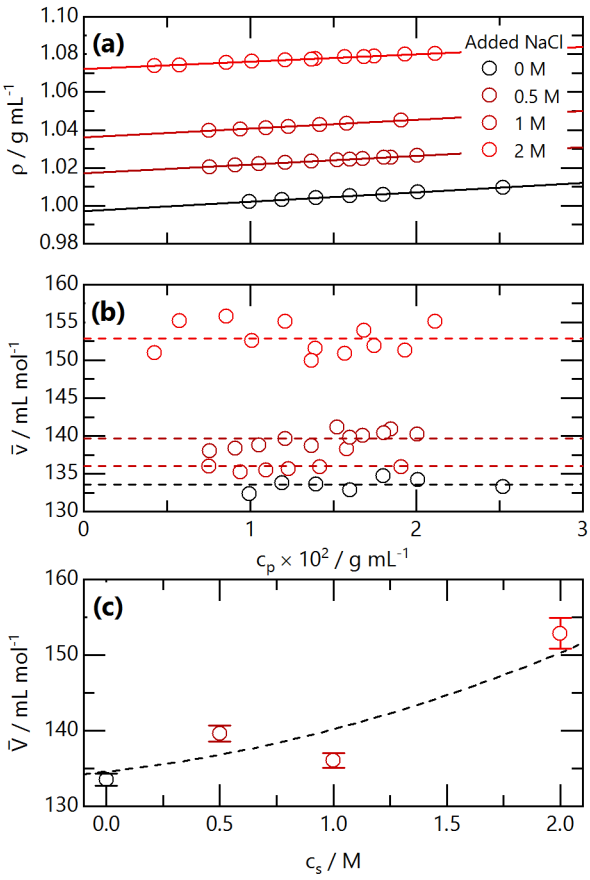

FIG. 13. (a) NaCMC solution density for solutions with 0-2 M added NaCl as a function of NaCMC concentration (in g mL^{-1}). Lines are linear fits to data with high statistical correlations ($R^2 > 0.99$) (b) Variation of apparent molar volume, determined from Equation 18 with NaCMC concentration. (c) Partial molar volume of NaCMC in NaCl solutions extracted from averages and standard deviation of the apparent molar volumes in (b). THe dashed line is a guide to the eye.

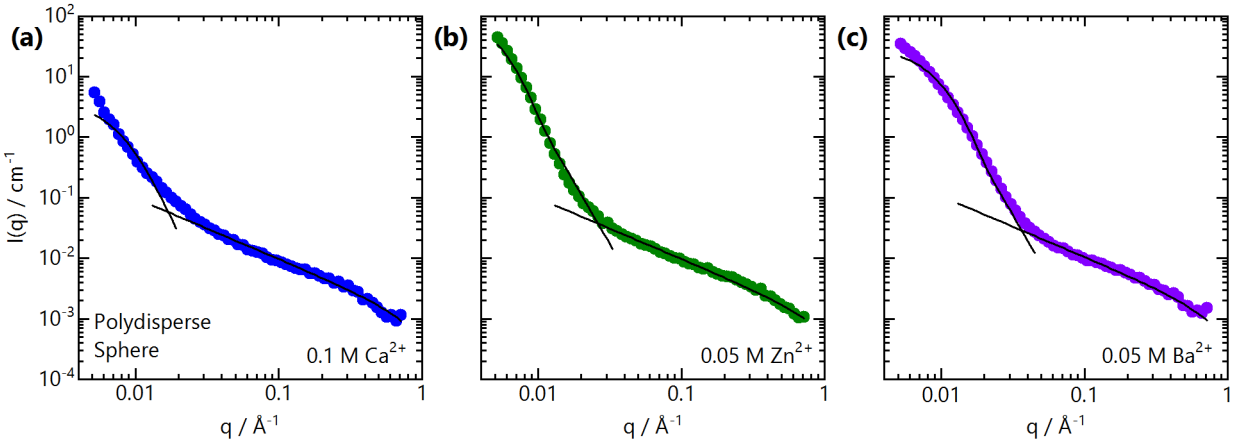

FIG. 14. 17.1 g L^{-1} ($\sim$ 64 mM) NaCMC with added (a) 0.1 M Ca^{2+} (b) 0.05 M Zn^{2+} (c) 0.05 M Ba^{2+}. Solid black lines are fits with a polydisperse spherical form factor at low-q and Equation 9 at high-q.

Cation	r_{sphere} / nm	PDI	$I_{0,High-q}$ / cm^{-1} $Å^{-1}$	R_c / Å	Intercept ($\frac{1}{\sqrt{I_0}}$) / $cm^{1/2}$	Slope ($\sqrt{\frac{\xi^2}{I_0}}$) / $Åcm^{-1/2}$	$\xi/Å$
Ca^{2+} (0.1 M)	18	0.3	9.75×10^{-4}	1.7	0.25 ± 0.05	11375 ± 490	214 ± 46
Zn^{2+} (0.05 M)	13	0.4	9.75×10^{-4}	1.5	-0.18 ± 0.03	9100 ± 150	223 ± 31
Ba^{2+} (0.05 M)	34	0.3	10.5×10^{-4}	1.8	0.05 ± 0.01	3535 ± 50	273 ± 54

TABLE III. Parameters used to fit polydisperse spherical form factor and high-q function in Figure 9 (a-c) and slope, intercept and correlation length extracted from Debye-Bueche plots in Figure 9 insets.

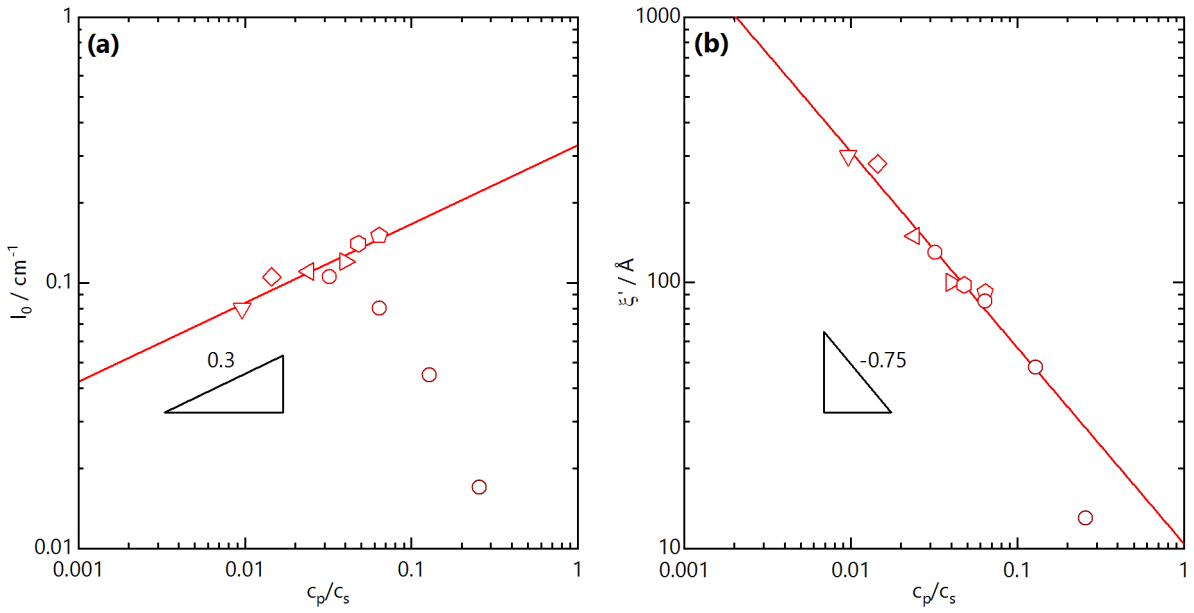

FIG. 15. (a) Correlation length ξ and (b) prefactor I_0 as a function of added salt concentration normalised NaCMC concentration for data at fixed excess added salt (2 M) and fixed polymer concentration (17.1 g L^{-1}) and variable added salt. Solid lines indicate power-law fits to the data.